Single-Photon Emission from Two-Dimensional Materials, to a Brighter Future

Sunny Gupta[1], Wenjing Wu[4], Shengxi Huang[4], and Boris I. Yakobson[1,2,3*]

[1]*Department of Materials Science and Nanoengineering, Rice University, Houston, TX, 77005 USA*

[2]*Department of Chemistry, Rice University, Houston, TX 77005, USA*

[3]*Smalley-Curl Institute for Nanoscale Science and Technology, Rice University, Houston, TX, 77005 USA*

[4]*Department of Electrical and Computer Engineering, Rice University, Houston, TX 77005, USA*

*Email: biy@rice.edu

TOC Image:

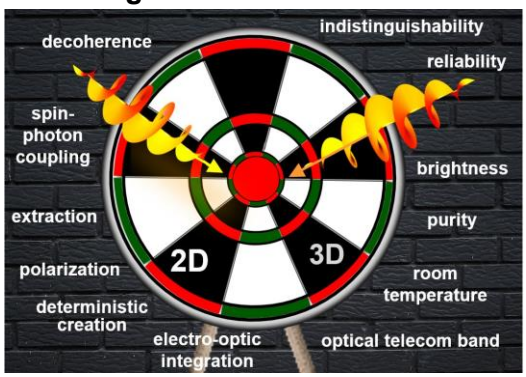

Abstract

Single-photons, often called flying qubits, have enormous promise to realize scalable quantum technologies ranging from an unhackable communication network to quantum computers. However, finding an ideal single-photon emitter (SPE) is a great challenge. Recently, two-dimensional (2D) materials have shown great potential as hosts for SPE that are bright and operate under ambient conditions. This perspective enumerates the metrics required for an SPE source and highlights that 2D materials, because of reduced dimensionality, exhibit interesting physical effects and satisfy several metrics, making them excellent candidates to host SPE. The performance of SPE candidates discovered in 2D materials - hexagonal boron nitride and transition metal dichalcogenides, will be assessed based on the metrics, and the remaining challenges will be highlighted. Lastly, strategies to mitigate such challenges by developing design rules to deterministically create SPE sources will be presented.

“And He said, 'Let there be light,' and there was light. God saw that the light was good…” The way we understand light has changed greatly over the centuries. From the ancient Greeks’ concept of light as a ray, to Newton’s corpuscular (particle) and Huygens’s wave theory, to the modern-day dual wave- and particle-like nature of light – made up of elementary particles with discrete energies called photons. Usually, the light we see from a prevalent source, say the Sun or an incandescent bulb, is polychromatic, incoherent, a gas of many photons with different energies. The light coming from a leaf, which we perceive as

green, is incoherent but almost monochromatic, having the majority of photons with similar energy. With the advent of lasers in the previous century, we were able to generate a monochromatic and coherent light in which all photons had the same energy (with very little broadening), revamping our knowledge of light. Recently, a new source of light called a single-photon emitter (SPE) has gained attention, as it produces just one photon at a time with a specific energy. Single-photons are quantum objects and can exist in two optical modes (of mutually perpendicular polarizations). Identical single photons which are indistinguishable from each other show quantum properties, such as entanglement - where two particles act like a single unit even when they are separated, and superposition - where a new quantum state can be created by a linear combination of other distinct quantum states. Experiments with single photons have affirmed[1] our understanding of quantum theory, stimulated applications, recognized by the 2022 Nobel prize in physics[2]. Moreover, the two optical modes of single photons form a two-state quantum system and can act as quantum bits or *qubits*, basic units for different quantum technologies of enormous promise, such as a communication network whose security is unhackable, unbreakable[4], a computer able to discover new drugs and promising exponentially higher computational power for particular tasks[5], to name a few.

Google, IBM, and others have already demonstrated[6] prototypes of small qubit devices using superconducting circuits, however, the operating temperature of such systems is colder than deep space, and the error in encoded quantum information (decoherence) in large qubit devices is unmanageable, making scalability a big challenge. Until now several promising candidates have been considered for qubits such as ion traps, quantum dots, Josephson junctions, photons, nuclear spins in silicon, and nuclear spins in molecules[7]. Among all candidates, single-photon flying qubits have been considered one of the leading candidates for realizing scalable quantum information processing (QIP) technologies. Single-photon sources with just linear optic elements such as beam splitters, phase shifters, and photo-detectors were proposed to be sufficient to realize a standalone QIP-on-chip device[8,9]. Moreover, single-photons were also predicted to play a great part in scaling up current state-of-the-art quantum devices using ion traps[10]. Photons do not interact with each other, and qubits based on photons polarization can potentially operate at room temperature and readily integrate into existing fiber optic-based telecommunications infrastructure. Moreover, using the electron spin as a memory register and photons to couple distant memory nodes through spin-photon interfaces can allow the scaling up of qubits, making quantum networks a household reality in the foreseeable future.

For realizing both spin and photonic qubits in a single system the promising candidates are the crystalline imperfections – defects in a solid material (Fig. 1a), with their discrete electronic energy levels. These *artificial atoms* have well-defined spin states, easily couple to light, and generate single photons with well-defined polarization. In bulk materials, with wide bandgap like SiC[11] and diamond[12], an archetypal SPE-capable point defect example is NV defect – a nitrogen (N) substitution neighboring a carbon vacancy (V) in diamond, widely studied and having already been used for a proof of concept demonstration of qubits operation. However, several challenges[13] limit its widespread use, e.g., the yield of photon emission into the zero phonon line is low (<4%), spectral diffusion is significant, creating an array of coherently linked NV qubits is difficult, and the optical transition is not in the required optical telecommunication band (0.77-1.1 eV). Certainly, there is a need to find alternative solid-state quantum emitters.

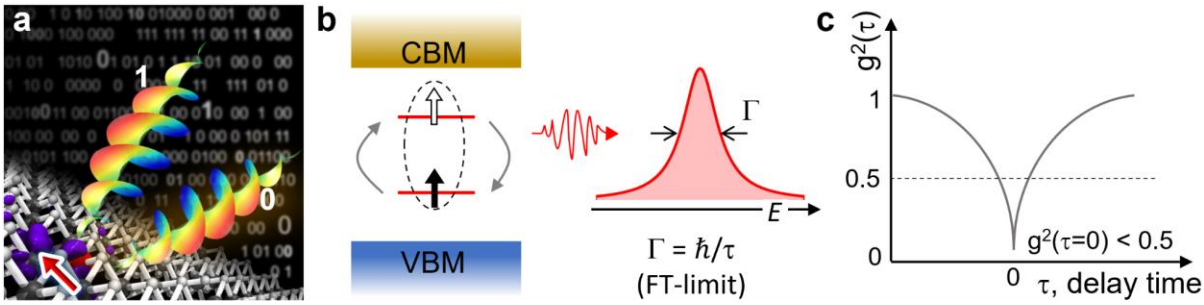

Fig. 1 (a) Materials defects with well-defined spin-state and consequently polarized single-photon emission, can be building blocks of spin-photonic qubit systems. (b) A schematic of a two-level system, which is paramagnetic, is well separated from the band edges and can emit single photons in the required Fourier transform (FT) limit, such that the broadening of emission in the spectral line Γ equals inverse of the excited-state decay lifetime $\Gamma = \hbar/\tau$. (c) A typical second-order photon correlation measurement plot $g^2(\tau)$, as a function of delay time τ, depicting antibunching (no more than one photon is emitted at a time). A value of $g^2(\tau=0) < 0.5$ is a signature of a "good" single-photon, as this quantity is connected to the probability of emitting two photons (or more) at the same time.

Two-dimensional (2D) materials, which are only *atomically thick*, have recently shown enormous promise as SPE host-media, imparting new meaning to Feynman's saying "*there's plenty of room at the bottom*". The interesting physical effects, arising from the reduced dimensionality of 2D layers, make them potentially on par or better, in certain cases, candidates to host SPE than bulk materials. Susceptible to environment perturbations due to their sub-nanometer thickness, 2D materials make it possible to position SPEs by external field engineering, deterministically. Although 2D material's atomic layer thickness offers engineering flexibility, it also renders the emitters prone to detrimental environmental perturbations. This perspective goes beyond the examination of the characteristics of various SPEs in 2D materials, covered in prior review articles[14–18]. The focus is on evaluating their performance based on several metrics for an ideal SPE. The metrics for an ideal SPE are outlined and the potential of 2D materials to meet these criteria is highlighted. The performance of various existing SPE candidates in 2D materials is compared to those in bulk materials using these metrics, with challenges and areas for improvement pinpointed. Lastly, strategies for mitigating such challenges through the development of design rules to create SPE sources deterministically is presented.

Requirements for ideal SPE? How satisfactory or promising a solid-state SPE is can be quantified by several metrics. (**i**) *Purity*, for which it must have a two-level quantum system with a ground state and an excited state (Fig. 1b), that can be perturbed by an external stimulus (light) to emit a single photon at a time with antibunching statistics (no more than one photon is emitted at a time), Fig. 1c. A measurement of second-order intensity autocorrelation function, $g^2(\tau)$, gauging the probability to emit two photons (or more) at the same time, serves a metric of purity. At zero delay time (τ = 0), a value of $g^2(\tau=0) < 0.5$ corresponds to antibunching, and is an important test for the quantum nature of SPEs. However, practical applications require $g^2(\tau=0) < 0.01$, more stringent[19]. (**ii**) Photons *indistinguishability*, requiring SPEs to have little spectral diffusion (variation in emitted photons wavelength) or, in other words, the spectral linewidth of an SPE (Γ) should be as low as the Fourier transform of its

excited state decay or called the lifetime T_1 of the emitter (Fig. 1b). For practical applications, indistinguishability requires the ratio $1/\Gamma T_1 > 0.99$[19]. A defect with inversion symmetry will be beneficial for this as it will suppress any defect coupling to stray electric fields that usually leads to spectral diffusion. (**iii**) *Brightness* (higher photon count), when the SPE excited state has short lifetime (that is high radiative rate, k_r)[19] and should maximally emit in the zero phonon line – ZPL, an emission due to electronic transitions only, without phonons. (**iv**) *Reliability* (high radiative efficiency)[19], i.e. the ground and excited states of two-level systems must be well separated in energy from non-radiative channels to any degenerate electronic states to which the two-level system can couple. (**v**) Minimal *decoherence*[20], requiring the defect levels to be isolated in energy from the host semiconductors' band edges and also be localized in real space, that is, have a smaller a_d – defect Bohr radius. (**vi**) *Polarized* emission, achieved by the two-level system being desirably fully polarized[19] in both absorption and emission channels and having a well defined photon quantum state. (**vii**) *Spin-photon coupling*, for which the defect must be paramagnetic, have a high spin-coherence time[20,21], and spin-states can be manipulated with light. (**viii**) Easy *extraction*, that is any internal reflection of single photons from the host must be avoided and emission direction must preferentially be unidirectional for maximizing collection efficiency[22]. (**ix**) *Deterministic creation* of the SPE centers at predefined locations[23,24] and easy *integration* into electro-optic circuits[25] and scalability. And lastly, (**x**) *Room temperature operation*[26] and emission in the *optical-telecommunications band*[11]. Although an ideal SPE would reach all the above metrics' extremes, in reality of the general Pareto principle, most definitive requirements for experimental demonstrations are (i-iv): *purity*, *indistinguishability*, *brightness*, and *reliability*. Other criteria like spin-photon coupling, room temperature operation, emission in optical-telecommunications band, and integration into electro-optic circuits, although not very critical, are still important to enable widespread applications.

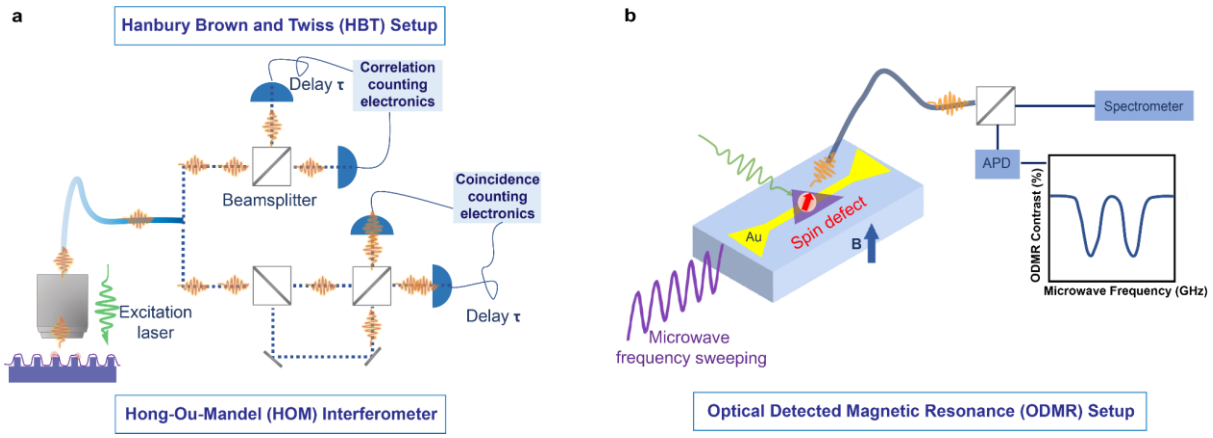

Fig. 2 Characterization of single-photon emitters. (a) SPEs generated in a strained 2D material layer on an array of nano-pillars and collected by a sequence of optics. Schematics of the Hanbury Brown and Twiss (HBT) setup for the measurement of purity $g^2(0)$ of the single photons and the Hong-Ou-Mandel (HOM) interferometer setup used to examine the indistinguishability of single photons. (b) Illustration of a typical Optically Detected Magnetic Resonance (ODMR) setup for spin state readout with optical pumping. A layer of 2D material (triangle) with spin active defects is placed on top of a gold waveguide, delivering a microwave for spin manipulation.

Experimentally, the important metrics for SPEs are assessed by different techniques. (i) For *purity*, a Hanbury Brown and Twiss (HBT) interferometer[27] (Fig. 2a), measuring the second order intensity autocorrelation function $g^2(\tau)$ is used. The $g^2(\tau)$ correlates intensities at

times differing by τ, measuring their joint detection probability. A classical light source of finite coherence time would exhibit positive correlations at a delay of $\tau \approx 0$ in the joint intensity detection probability, leading to bunching in the photon arrival time. Inversely, a single-photon (Fock) state has just one photon, for which $g^2(\tau = 0) = 0$ because no joint detection can take place. Hence, $g^2(\tau)$ has become a measure of the single-photon source purity. A value of $g^2(\tau=0) < 0.5$ corresponds to antibunching, an important metric for the quantum nature of SPEs. (ii) For *indistinguishability*, the two-photon Hong-Ou-Mandel (HOM) interference[28] (Fig. 2a) detects the well-defined spatial and temporal modes inherent to a good SPE. When two indistinguishable single-photons enter a 50:50 beam splitter, one in each input port, they will always exit the beam splitter together in the same output modes. The probability of both photons exiting separately is zero because of destructive interference, and the coincidence count of exiting photons at zero time delay will ideally be zero. Measuring such coincidence count, HOM interferometer determines the indistinguishability of the single photons. (iii) For *brightness*, representing the photon generation ability – usually expressed by the product of the excitation pulse rate, quantum yield and the collection efficiency of the system – experimental characterization is done by photoluminescence (PL) or electroluminescence (EL) spectroscopy. (iv) For *reliability*, its metrics can be represented by the radiative lifetime, emission temperature, and spectral wandering/blinking. Some 2D SPEs are spin active, this additional degree of freedom enabling the optical manipulation and readout of spins, which can be utilized in quantum photonic circuits. Optically detected magnetic resonance (ODMR)[29] (Fig. 2b) and electron paramagnetic resonance (EPR) spectroscopy can effectively characterize the nature of spin-active defects.

Why are 2D materials potentially better hosts for SPE? The reduced dimensionality of 2D materials helps in dealing with several challenges faced by existing photon sources, such as trapped single molecules, quantum dots, and NV centers in diamond, and naturally satisfies several of the above metrics. Due to the quantum confinement effect and reduced screening in 2D, several requirements for ideal SPE mentioned above can be satisfied: (**iii**) the radiative rate (k_r) and the oscillator strength (f_{osc}) of the optical transition between defect electronic levels are likely to be higher in 2D[30] ($k_r \propto f_{osc} \propto 1/a_d^3$), (**iv**) it was shown that the defect-phonon interaction responsible for Franck Condon shift in 2D transition-metal dichalcogenides (TMDC) is small[31], which enhances radiative efficiency of the transitions, (**v**) defect states are more isolated from the band edges in 2D materials and have smaller Bohr radius[30] ($a_d \propto \varepsilon$, ε being the dielectric constant), (**vii**) the theoretically predicted spin coherence time is longer in 2D, ref. [21,32], (**viii**) the all-surface openness and optical transparency of 2D materials facilitate easy photon extraction, and (**ix**) their planarity helps atomic-precision control of defects and their heterogeneous integration with electro-optic circuits. Moreover, the unique architecture of 2D materials makes the SPE-modules easier to integrate with various optical cavity structures, which is crucial for scalability and realizing on-chip photonic devices. All these attributes of defects in 2D semiconductors make them promising host candidates for SPE.

Despite the advantages of 2D host materials, research of these systems is still in its infancy, and practical applications require finding a nearly ideal, best possible SPE satisfying at least the most practical, if not all of the above metrics. Recently, SPEs have been observed in several 2D materials, like hexagonal boron nitride (hBN) and TMDCs. Next, we briefly review the progress among such candidates and assess their performance according to the above metrics.

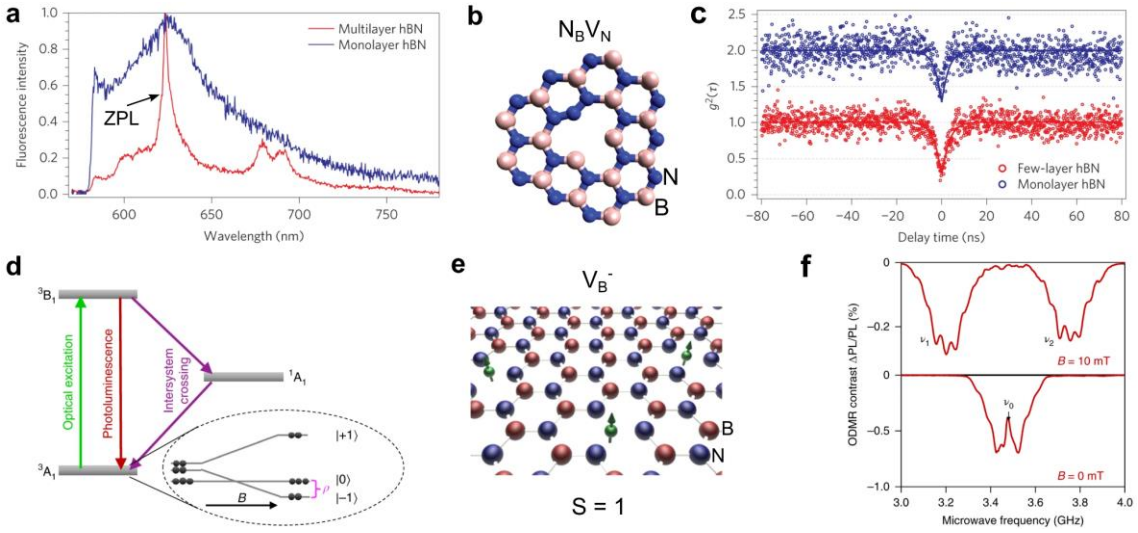

Fig. 3 Single-photon emitters in hBN. (a) Room-temperature photoluminescence spectra of a defect center in hBN monolayer (blue) and multilayer (red). The arrow points to the zero phonon line (ZPL) emission peak. (b) Defect structure of one of the possible candidates for SPE in hBN, N_BV_N, where nitrogen is substituted at boron site with a neighboring nitrogen vacancy. (c) A signature of single-photons are the antibunching curves $g^2(\tau)$, offset vertically for clarity, from an individual defect in hBN monolayer (blue circles) and multilayer (red circles), corresponding to the spectra in (a). Emitters in hBN with optically addressable electron spin state (d-f) demonstrated by optically detected magnetic resonance (ODMR). (d) Simplified energy-level diagram illustrating the optical pump cycle between ground state $^3A_1$, excited state $^3B_1$ and metastable state $^1A_1$, resulting in the ODMR contrast. Optical excitation (green), PL (red) and intersystem crossing (purple) are indicated by arrows. (e) A possible defect with spin triplet (S=1) ground state responsible for the signals, V_B^-, a charged boron vacancy. (f) ODMR spectra measured at zero magnetic field (bottom) and at magnetic field B = 10 mT (top) with the ODMR frequencies ν_0, ν_1 and ν_2, corresponding to states with m_s = 0, -1, and +1, respectively. The microwave-induced magnetic dipole transitions between spin sublevels manifest as changes in PL intensity (ΔPL) and result in ODMR contrast, which signifies preparation of well defined spin states. Panels a-c are adapted from ref.[33], Springer Nature Limited. Panels d-f are adapted from ref.[34], Springer Nature Limited.

Single-photon emitters in hBN - Hexagonal boron nitride (hBN) is an insulator with a large band gap of ~6 eV. Few-layer hBN is one of the most studied 2D materials as a host for SPEs. Defects in hBN with electronic levels in the band gap have been ascribed as the likely source for SPE with ZPL energies ranging in the NIR-visible range ~1.6–2.2 eV[33,35] (Fig. 3a) and the UV range ~4.1 eV[36]. The single-photon nature of the emissions was confirmed by measuring the $g^2(\tau)$ via HBT interferometry. At zero delay time (τ = 0), a value $g^2(\tau=0) < 0.5$ (Fig. 3c) corresponds to antibunching, an important evidence of the quantum nature of SPEs, thereby satisfying metric (i). The emission has been observed at room temperature, similar to that in bulk diamond[37] and SiC[26], satisfying metric (x) as well. The SPEs in hBN also have a larger Debye–Waller (DW) factor (~0.82) compared with that of NV centers (~0.13). DW factor is the ratio of the ZPL intensity to the total emission, and is connected with metric (iii) for ideal SPE. A large DW factor corresponds to high photon count and SPEs in hBN are naturally very bright (without any Purcell enhancement[38]) with photon-counts 10^6 Hz or more[33]. The polarized nature of single-photons, combined with the weak electron–phonon coupling and exceptional chemical and photostability[33,35] of SPEs in hBN, makes them very promising sources for quantum emission. Some SPEs in hBN have also shown a magneto-optical effect[34,39]

consistent with an optically addressable electron spin state (Figs. 3d-f), adding a potential for spin-photonic qubits.

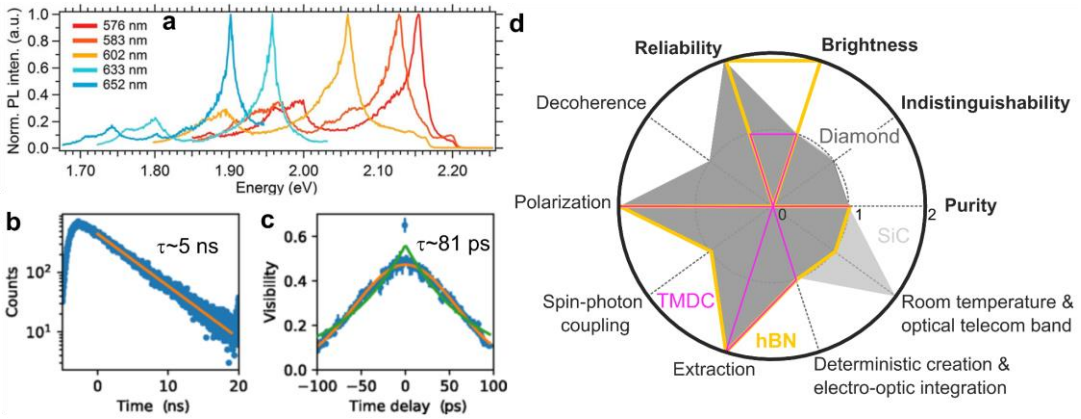

Fig. 4 Challenges with quantum emitters in hBN. (a) Emitters in hBN showing large spectral variation of ~0.3 eV. Lifetime and coherence measurements of a single defect in hBN (b-c). (b) Lifetime measurement, blue for data and orange for exponential fit with τ_{lf} = 4.93 ns. (c) Measured first-order coherence: blue is data, green is exponential fit at $\tau_{c,e}$ = 76 ps, orange is Gaussian fit at $\tau_{c,G}$ = 81 ps. The inequality τ_{lf} >> $\tau_{c,G}$ means that the emitted signal is not FT-limited -- a condition for photon indistinguishability. The $\tau_{c,G}$ = 81 ps value translates to a width of ~6.5 GHz which is higher than the FT-limited ~32 MHz obtained from τ_{lf} = 4.93 ns. (d) A rose diagram compares the defects in diamond, SiC, hBN, and TMDCs based on the 10 SPE metrics. The values of 0, 1, or 2, corresponds to the metric being not seen, seen but to be improved, or meeting requirements, respectively. The 4 most important metrics are in bold. Panel a: Reprinted with permission from ref.[35]. Copyright 2017, American Chemical Society. Panel b-c: Reprinted with permission from ref.[40]. Copyright 2017, American Physical Society.

Although some of the metrics for quantum emitters in hBN appear satisfactory in a rose diagram Fig. 4d, several challenges have thwarted their widespread exploration. The factual atomic structure of SPE in hBN remains ambiguous. Indeed, the ZPL energies widespread from visible to UV, signify that there are likely multiple defects responsible for SPE. Indeed, the defects are created randomly by the electron-beam irradiation and annealing[35], optimized but without much control of their position and type. This makes consistent progress and validation of results among different studies very difficult, as compared with NV centers in diamond. (Theoretical studies suggest several possible candidates for SPE in hBN including C_BV_N (ref. [30,41]), $V_BC_N^-$ (ref. [42]), N_BV_N (ref. [33,43], Fig. 3b), V_B^- (ref. [43], Fig. 3e), dangling bonds[44]. However, none have been fully ascertained in experiments. In a single sample, the random SPEs created have a large spectral variation of ~0.3-0.4 eV[35] (Fig. 4a), degrading the indistinguishability of emitted photons. The variations were earlier attributed to local inhomogeneities in strain and dielectric environment[35]; however, strain is recently found not responsible[45] for the spectral variations, while the structural and chemical distinction of the defects might play a role, thereby adding more haze to the uncertainty in the microscopic origin of SPEs. Spectral tuning of SPEs by strain[46] or Stark effect in electric field[47] has been attempted, but the tunability window is limited. Even in a selected SPE, the emitted photon is found to have large spectral diffusion[40] arising from inhomogeneous broadening, which gives linewidths much larger than FT limited values (Fig. 4b-c), thereby limiting the photons indistinguishability. The excited-state lifetime of SPEs is ~4.9 ns (Fig. 4b), giving the target FT-limited natural linewidth of $(2\pi\tau)^{-1}$ ≈ 32 MHz (0.1 μeV), much smaller than typically

observed ~6500 MHz. The spectral diffusion is hypothesized to arise from the spectral jumps of SPE due to fluctuations in the local electric field, caused by changes in nearby impurities and environment[40]; admittedly, a clear understanding is still lacking. Exploring comprehensively the role of changes in dielectric substrates, encapsulation, and atmosphere on spectral diffusion, must eventually shed more light on the microscopic causes and mitigation strategies. Integrating the SPEs in hBN to optical cavities and photonics platforms, which is a prerequisite to scalability, and an additional increase in emission rates, enhanced collection efficiency, and linewidth reduction are all underway[25]. However, coupling optical cavities to single isolated SPE is still a challenge.

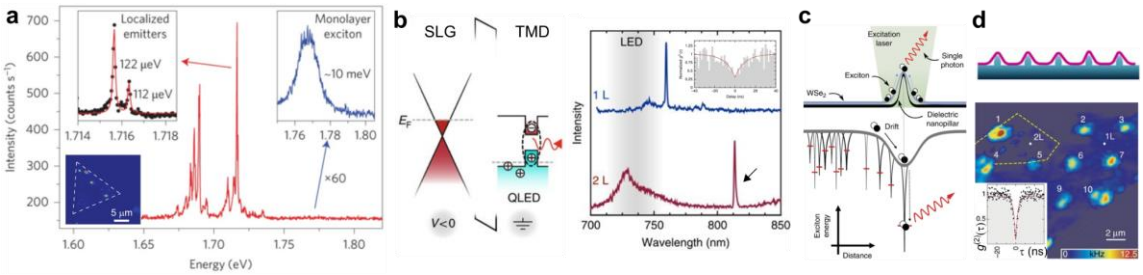

Fig. 5 Single-photon emitters in TMDCs. (a) PL spectrum of localized emitters at 4.2 K in WSe_2. The insets are the zoom-in of the localized emitters (left), emitting much sharper than the monolayer valley exciton (right). The bottom left inset is the PL-intensity map of narrow SPE lines localized mostly near material-triangle edges. (b) Electrical generation of single-photons. On the left is the heterostructure band diagram. Under a negative bias applied to the single layer graphene (SLG), its Fermi level (E_F) crosses the TMDC conduction band edge, allowing electron tunneling SLG $-e^-\rightarrow$ TMDC. The electron, trapped at quantum dots in TMDCs, recombines with holes, to emit a single-photon. The right panel shows the electroluminescence (EL) emission spectra for quantum dots in the monolayer (top) and bilayer (bottom) WSe_2. The shaded spectral window is for LED emission due to bulk WSe_2 excitons, whereas the arrow shows the longwave emission from quantum dots. Strain-induced quantum emission from TMDCs on patterned substrates (c-d). (c) Atomically thin WSe_2 on a nanopillar (top) attains a point-like elastic strain (bottom), modulating the WSe_2 band gap. Superimposed on this artificial modulation of the exciton energy are randomly located excitons. Optically created excitons funnel to an individual strain-localized trap at the nanopillar tip resulting in a single highly efficient quantum emitter. (d) Top schematic, placing a 2D material on periodic nanopillars deterministically creates quantum emitters. Bottom, a color-coded spatial map of the peak PL signal greatest at the pillar locations. Panel a is adapted from ref.[48], Springer Nature Limited. Panel b is adapted from ref.[49], Springer Nature Limited. Panel c is adapted from ref.[23], Springer Nature Limited. Panel d is adapted from ref.[50], Springer Nature Limited.

Single-photon emitters in TMDCs - TMDCs are another widely studied class of materials, where SPE has been observed[48,51–53]. WSe_2 was one of the first examples, its SPEs attributed to excitons localized at defects, with the observed emission lines 10-200 meV below the free 2D excitons (Fig. 5a), confirmed antibunching, the ZPL linewidths under 150 μeV, while the excited-state lifetime ~1-2 ns was comparable to hBN. The emission was polarized, showing large Zeeman effects, with a high excitonic *g*-factor of 7-12 and zero magnetic field spectral splitting of ~1 meV. This suggested that SPEs are caused by neutral excitons trapped at anisotropic confining potentials from defects in the monolayer[48]. Interestingly, the single-photons in WSe_2 and WS_2 were also found to be generated electrically[30,33] (Fig. 5b), which is technologically very attractive: the carriers injected into TMDCs conduction band, controlled by an external voltage, appear trapped at defects, to emit single-photons. Additionally, strain

fields from placing TMDCs on substrate patterned with pillars were also used to generate single-photons[23,50,54,55] (Fig. 5c-d). This allowed deterministic placement of SPEs, which is very appealing for scalability. Placing a 2D material on a nonplanar topography, such as a nano-pillar, with non-zero Gaussian curvature, generates strain fields[56,57], which funnels free 2D excitons to its site. The migrated excitons can get trapped at nearby defects and thus emit single-photons (Fig. 5c).

Apart from W-based TMDCs, SPEs have been realized in Mo-based monolayer and few-layer ditelluride ($MoTe_2$)[58] by site-controlled strain engineering. The SPE emission showed 90% single-photon purity, and the photon antibunching behavior lived up to 77 K. In MoS_2[59] and $MoSe_2$[60] monolayers, SPEs have also been achieved with defect and strain engineering. Recently, SPE has been observed in a moiré system[61] of two TMDC layers with a twist angle, creating a superlattice with a periodic potential landscape, which traps interlayer excitons, emitting single photons. These SPEs show tunability in the presence of an external electric field, electrostatic gating, and local strain. The SPE emission energy can be tuned by ~40 meV due to the Stark effect in the vertical electric field. SPEs have also been observed in other types of 2D materials, such as metal chalcogenides and oxides. GaSe with intrinsic local selenium cluster intercalation has been proven to host localized excitons and biexcitons up to room temperature[62]. Heterogeneities from transforming WSe_2 flakes into cubic WO_3 by thermal annealing also host room-temperature SPEs[63].

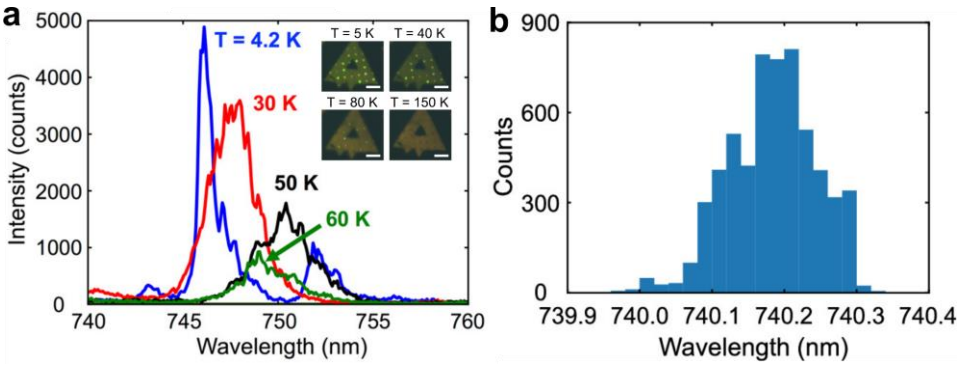

Fig. 6 Challenges with quantum emitters in TMDCs. (a) The photoluminescence from SPEs in TMDCs, placed on patterned indentations, diminishes in intensity when raising temperature. The fluorescence image at different temperatures (inset) reveals limited temperature operability. (b) Spectral wandering in the emission wavelength. Panel a,b: Reprinted with permission from ref.[54] Copyright 2019, American Chemical Society.

Although the research on SPEs in TMDCs has significantly progressed after its discovery in 2015, they underperform in several metrics (Fig. 4d). All SPEs in TMDCs only operate at cryogenic and low temperatures (Fig. 6a), limiting their use. Similar to hBN, the microscopic nature of defects responsible for single-photons in TMDCs remains unclear. The ZPL linewidths observed are large and FT-limited signals have not been seen due to significant spectral diffusion (Fig. 6b). Moreover, the brightness (photon count rate)[52] of ~kHz is way below that in hBN. To increase the operational temperature, a few techniques such as coupling of SPEs to plasmonic cavities[64], and creating defects with deep electronic levels by electron-beam irradiation[65] have been attempted. Tuning of SPEs by quantum-confined Stark effect was achieved in WSe_2 monolayer[66]. Furthermore, electrostatic switching of SPEs in MoS_2 was realized in a field-effect device, showing that the SPEs are sensitive to charge carrier concentration, similar to free excitons[67].

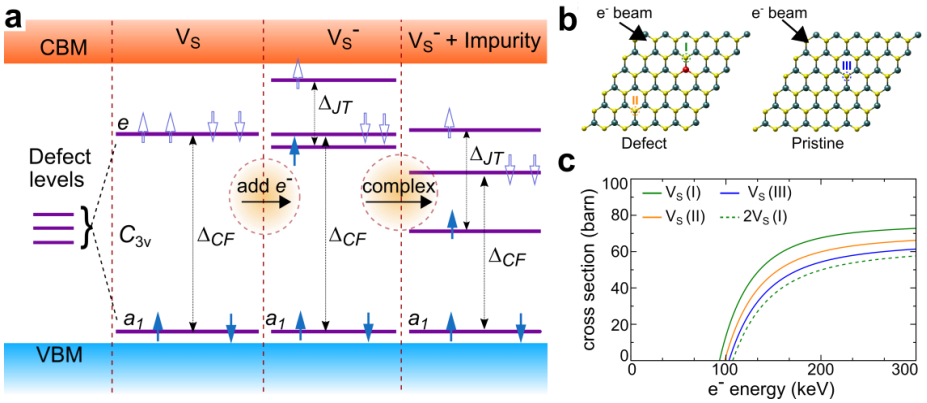

Fig. 7 Deterministic creation of SPEs in 2D materials. (a) Schematic describing the design strategy of creating point defects with two-level systems. Electron energy levels in a point defect (vacancy) split according to its symmetry. V_S defect has C_{3v} symmetry and its states split into a_1 (occupied) and e (empty) levels due to the crystal field (CF) of the host. The defect is nonparamagnetic, therefore an extra e^- in V_S (charged defect) further splits the e-levels due to JT distortion and creates a two-level system. The energy levels are not isolated from band edges making them not optimal for SPE. Added paramagnetic impurity forms a defect complex ($Re_{Mo}V_S$), adds an extra e^- to the neutral V_S and perturbs both CF and JT energies, creating a two-level system. Thus, adding a paramagnetic impurity next to a vacancy defect must be conducive to creating a two-level system. (b) Location of V_S sites in MoS_2 with Re_{Mo} defect adjacent to it, far away, and in pristine MoS_2. The calculated displacement threshold energy (T_d) of sputtering a sulfur atom from these sites. (c) Cross section for different sites shown in (b) versus incident e^- beam energy. $2V_S$ means creation of divacancy. The energy to create V_S near Re_{Mo} is smaller than for other locations. Panel a,b,c: Reprinted with permission from ref.[30] . Copyright 2019, American Chemical Society.

Outlook - Already available facts of observations as well as theoretical understanding leave no doubts that 2D materials can host excellent sources for single photon emission – in principle. However (attributed to Yogi Berra), "In theory, there is no difference between theory and practice. In practice, there is." Indeed, one of the major challenges facing SPEs realization in 2D materials is to understand what the single photons-emitting defects really are, in terms of atomic structure, in order to advance their oftentimes erratic formation towards deterministic engineering. This is required for merely comparing and validating results from different laboratories and further for achieving scalability of SPE sources. Such advances should allow SPEs in 2D materials to gain the same level of attention and enthusiasm as received by archetypal NV and similar defects in diamond crystals. Although the research on exploring properties of SPEs in 2D materials has progressed significantly, there is a need to take a pause and address challenges, sequentially, and not just jump on the bandwagon. Firstly, one must formulate a bottom-up strategy and design rules for identifying defects in 2D materials that are desirable for SPE. One such general design strategy to create practical two-level systems in 2D materials for SPE was recently formulated[30]. Despite being applied to 2D systems, this approach[30] is versatile and can be used to construct two-level systems even in 3D bulk materials. It was theoretically shown that adding a paramagnetic impurity adjacent to a vacancy defect can create two-level systems in a variety of 2D materials. This strategy was demonstrated by taking the V_S defect in MoS_2, and perturbing its defect levels by the adjacent Re_{Mo}, forming a $Re_{Mo}V_S$ defect complex, with paramagnetic states and two-level systems that

are well separated from the band edges. The approach appears general, and firstly involves recognizing the point group symmetry of the initial defect to identify its electronic levels, as shown by e and a_1 levels for V_S defect of C_{3v} symmetry (Fig. 7a). Subsequently, if the defect does not display two-level systems, then the occupancy of the electronic levels and their splittings can be engineered, to perturb the crystal field Δ_{CF} and Jahn-Teller splitting Δ_{JT}, by combining V_S with a paramagnetic impurity like Re_{Mo}. This general strategy was then used to create, in accurate computational models, similar kinds of defects in different 2D materials including TMDCs, hBN, and even 2D diamond (diamane, an emergent material[68,69] attractive as a 2D platform for the already credible SPE as NV-defects). It was also predicted that these defects can be deterministically created by a two-step process. Firstly, dope a general 2D material MX_2 with atoms R such that it has one extra valence electron and lies to the right of atoms M in the periodic table. Such doping has already been demonstrated[70] in different 2D materials. Secondly, irradiate the doped sample with e^--beam to create a V_X defect near R_M so to form a complex R_MV_X. The energy threshold to create V_X defect adjacent to R_M was calculated to be lower than anywhere else in the crystal (Fig. 7b,c) and thus R_MV_X defects can be created nonrandomly, in a controllable fashion. This strategy can be employed for deterministic creation of defects in a variety of TMDC and other 2D materials and should lay a strong foundation for further explorations. High-throughput computations[71] and machine-learning[72] approaches are also being used to predict and identify defects with best properties. To satisfy other metrics of SPE, a combined theoretical and experimental (co-design) approach is required. The theory guides experiments by recommending the best choices and experiments providing feedback to refine theoretical parameters and guiding rules. Several key parameters like exciton lifetime, optical spectra including absorption and photoluminescence, spin relaxation time (T_1), spin decoherence time (T_2), as well as Huang-Rhys factor can be theoretically calculated for defects from first-principles[73] and quantitatively compared with experiments. Such co-design strategies have been applied to understand defect related emission in MoS_2[74], and hBN[42]. Moreover, research into deterministically creating SPE sources via a bottom-up synthesis method is currently underway[42], but much more work is required. Ion-implantation[75], which is an effective way to deterministically create SPEs in bulk materials like diamond, can also be employed on 2D materials. Some work is underway as SPEs were observed in monolayer MoS_2 sandwiched between the top and bottom hBN layers, and irradiated with helium ions at specific positions[59,76]. Focused ion beam (FIB) milling of hBN created a patterned array of SPEs with a yield of 31%[24]. Moderate electron beam[77] and femtosecond laser[78] irradiation, chemical etching[79], and more recently a combination of twisting bilayers and e^- beam irradiation[80] have also successfully created SPEs in TMDC and hBN with site specification.

Once these defects are created deterministically, their density can be controlled as well. Ideally one must select defect candidates, which have inversion symmetry to minimize coupling to stray electric fields, which is one of the main reasons for linewidth broadening and prevents FT-limited emissions and photon's indistinguishability. Furthermore, coupling the SPEs to well-designed cavities with Purcell enhancement can further reduce the lifetime, such that the linewidths become comparable to inverse lifetime and FT-limited signals with indistinguishable photons are achieved. To achieve a high photon count, one must select defects with large DW factors, which can be theoretically calculated for different candidates prior to experimental syntheses. Additionally, coupling the emitters to optical cavities can also enhance the emission rates and photon counts. It is of technological interest to search for SPEs with emissions in the optical telecommunications bands. This can be achieved by

studying defect complexes similar to R_MV_X in materials such as Pt and Zr-based TMDCs. The variations in the substrates, where the 2D materials are placed, also affects the electronic levels of the defects[81] via changes in the effective dielectric environment. This aspect, unique to 2D materials must also be taken into account when designing SPEs.

Understanding decoherence of SPEs in 2D materials is another major challenge. Electron-phonon interaction between the localized carriers and the host material lattice is believed[82] to have a non-trivial contribution to the decoherence of the SPEs in 2D materials. At elevated temperatures, the emission from TMDC SPEs quenches significantly, due to the depopulation of quantized states resulting from the electron-phonon coupling. Thus room temperature functioning 2D SPEs mainly exist in hBN owing to its large bandgap, which helps isolate the defect transition from the band edge transition, even with thermal fluctuation. Other types of decoherence mechanisms include the electron-nuclei spin interaction between the localized carriers and the substrate defect such as dangling bonds and dynamic environment depending on the interface disorder. Significant efforts[83–85] have been made to overcome the decoherence. hBN encapsulation of TMDC samples can help screen the dielectric disorder. High-quality intrinsic crystal with controlled defect density is another effective choice. And devices with electrical control have the ability to deplete the excess carriers in the system.

In reality, searching for SPEs in 2D material devices is rather time-consuming, though site-specification attempts with strain engineering have been made. An efficient and accurate way to characterize SPEs is highly demanded. Fast photoluminescence mapping of the emission intensity and linewidth is the first step in identifying SPEs. Machine learning algorithms which can quickly analyze the mapping data and identify highly possible SPE 'hot spots' is desirable[86]. Additionally, measuring the photon correlation for rapid classification of SPEs in autocorrelation measurement is being realized with machine learning[87]. Practical applications require the generated single photons to be efficiently read and manipulated, however, these have not been achieved yet in 2D materials. Efficiently capturing[22] the emitted photon having a broad angular distribution with a high probability is yet to be demonstrated. The emitted photons must be indistinguishable from each other and preserving the coherence in qubits within 2D materials, especially flying qubits that need to be transmitted to long distances poses a substantial challenge. 2D materials are sensitive to their surroundings and can be readily impacted by thermal and electromagnetic disturbances, leading to decoherence and the subsequent loss of quantum information. Consequently, devising strategies to manipulate and enhance the coherence duration of qubits in 2D materials, as has been applied[88] to defects in bulk materials, is crucial for the successful integration of flying qubits.

Achieving all the metrics' (i-x) extremes for an SPE is practically unfeasible. The near term goal should be to at least satisfy the following conditions[19] essential for specific applications. (a) for *quantum key distribution*, QKD: Purity <0.1, Indistinguishability: not critical, Reliability (efficiency) >0.5, Brightness >GHz. (b) for *quantum computing*: Purity <0.001, Indistinguishability >0.99, Reliability (efficiency) >0.99, Brightness >GHz. (c) for *memory-based quantum repeaters*: Purity <0.01, Indistinguishability >0.9, Reliability (efficiency) >0.9, Brightness >GHz.

Conclusions - We highlighted that 2D materials, by virtue of reduced dimensionality, have several fundamental advantages, which makes them excellent host candidates for SPE. Room temperature operation, high-photon count (brightness), electrically triggered generation, low excited-state lifetime, polarized emission, and optically addressable electron spin state, are

some of the features already shown by SPEs in 2D materials, which in far sight appears that single-photon emitters in 2D materials have a bright future. The microscopic nature of defects responsible for SPEs, their deterministic creation, and the indistinguishability of emitted photons are important metrics that have not been demonstrated yet. There is a need to use a bottom-up approach and combine theoretical and experimental knowledge first to identify a few best defects that the whole community can explore together, similar to research on NV centers in diamond. Subsequently, combining SPEs with optical cavities and photonics platforms on a single chip will improve the brightness, stability, indistinguishability of the emitters, and scalability to achieve an on-demand source of indistinguishable single-photons operating at room temperature.

Biographies

Dr. Sunny Gupta is a postdoctoral scholar in the Materials Science and Engineering department at University of California, Berkeley and Lawrence Berkeley National Laboratory. He earned his PhD degree in Materials Science and Nanoengineering at Rice University in 2021. His research interests are theory and design of functional quantum materials and materials for energy applications.

Wenjing Wu is a Ph.D student majoring in applied physics at Rice University. Wenjing works at the Sensing, Characterization and Optoelectronics Lab in the Department of Electrical and Computer Engineering, and her research mainly focuses on optical properties of low-dimensional quantum materials.

Dr. Shengxi Huang is an assistant professor in the Department of Electrical and Computer Engineering at Rice University. Shengxi earned her PhD degree in Electrical Engineering and Computer Science at MIT in 2017. Following that, she did postdoctoral research at Stanford University. Her research interests involve light-matter interactions of quantum materials and nanostructures, as well as the development of new quantum optical emission platforms.

Dr. Boris I. Yakobson is a Karl F. Hasselmann Endowed Chair Professor of Engineering, a professor in the Department of Materials Science & NanoEngineering and in the Department of Chemistry of Rice University. He earned his PhD in Chemical Physics and Applied Mathematics from the Russian Academy of Sciences in 1982. He moved to the US in 1989 and joined Rice University in 1999. His research interests are in theory of materials, of their synthesis/growth, defects, structural-mechanical, electronic, and optical properties.

References

(1) Freedman, S. J.; Clauser, J. F. Experimental Test of Local Hidden-Variable Theories. *Phys. Rev. Lett.* **1972**, *28* (14), 938–941. https://doi.org/10.1103/PhysRevLett.28.938.

(2) *The Nobel Prize in Physics 2022*. NobelPrize.org. https://www.nobelprize.org/prizes/physics/2022/press-release/ (accessed 2022-10-06).

(3) Barry, J. F.; Turner, M. J.; Schloss, J. M.; Glenn, D. R.; Song, Y.; Lukin, M. D.; Park, H.; Walsworth, R. L. Optical Magnetic Detection of Single-Neuron Action Potentials Using Quantum Defects in Diamond. *Proc. Natl. Acad. Sci.* **2016**, *113* (49), 14133–14138. https://doi.org/10.1073/pnas.1601513113.

(4) Naik, D. S.; Peterson, C. G.; White, A. G.; Berglund, A. J.; Kwiat, P. G. Entangled State Quantum Cryptography: Eavesdropping on the Ekert Protocol. *Phys. Rev. Lett.* **2000**, *84* (20), 4733–4736. https://doi.org/10.1103/PhysRevLett.84.4733.

(5) Cao, Y.; Romero, J.; Aspuru-Guzik, A. Potential of Quantum Computing for Drug Discovery. *IBM J. Res. Dev.* **2018**, *62* (6), 6:1-6:20. https://doi.org/10.1147/JRD.2018.2888987.
(6) Arute, F.; Arya, K.; Babbush, R.; Bacon, D.; Bardin, J. C.; Barends, R.; Biswas, R.; Boixo, S.; Brandao, F. G. S. L.; Buell, D. A.; Burkett, B.; Chen, Y.; Chen, Z.; Chiaro, B.; Collins, R.; Courtney, W.; Dunsworth, A.; Farhi, E.; Foxen, B.; Fowler, A.; Gidney, C.; Giustina, M.; Graff, R.; Guerin, K.; Habegger, S.; Harrigan, M. P.; Hartmann, M. J.; Ho, A.; Hoffmann, M.; Huang, T.; Humble, T. S.; Isakov, S. V.; Jeffrey, E.; Jiang, Z.; Kafri, D.; Kechedzhi, K.; Kelly, J.; Klimov, P. V.; Knysh, S.; Korotkov, A.; Kostritsa, F.; Landhuis, D.; Lindmark, M.; Lucero, E.; Lyakh, D.; Mandrà, S.; McClean, J. R.; McEwen, M.; Megrant, A.; Mi, X.; Michielsen, K.; Mohseni, M.; Mutus, J.; Naaman, O.; Neeley, M.; Neill, C.; Niu, M. Y.; Ostby, E.; Petukhov, A.; Platt, J. C.; Quintana, C.; Rieffel, E. G.; Roushan, P.; Rubin, N. C.; Sank, D.; Satzinger, K. J.; Smelyanskiy, V.; Sung, K. J.; Trevithick, M. D.; Vainsencher, A.; Villalonga, B.; White, T.; Yao, Z. J.; Yeh, P.; Zalcman, A.; Neven, H.; Martinis, J. M. Quantum Supremacy Using a Programmable Superconducting Processor. *Nature* **2019**, *574* (7779), 505–510. https://doi.org/10.1038/s41586-019-1666-5.
(7) Braunstein, S.; Hoi-Kwong, L. Experimental Proposals for Quantum Computation-Foreword. *Fortschritte der Physik* **2000**, *48*, 767–1138.
(8) Knill, E.; Laflamme, R.; Milburn, G. J. A Scheme for Efficient Quantum Computation with Linear Optics. *Nature* **2001**, *409*, 46–52. https://doi.org/10.1038/35051009.
(9) Kok, P.; Munro, W. J.; Nemoto, K.; Ralph, T. C.; Dowling, J. P.; Milburn, G. J. Linear Optical Quantum Computing with Photonic Qubits. *Rev. Mod. Phys.* **2007**, *79*, 135–174. https://doi.org/10.1103/RevModPhys.79.135.
(10) Monroe, C.; Kim, J. Scaling the Ion Trap Quantum Processor. *Science* **2013**, *339* (6124), 1164–1169. https://doi.org/10.1126/science.1231298.
(11) Lohrmann, A.; Johnson, B. C.; McCallum, J. C.; Castelletto, S. A Review on Single Photon Sources in Silicon Carbide. *Rep. Prog. Phys.* **2017**, *80* (3), 034502. https://doi.org/10.1088/1361-6633/aa5171.
(12) Aharonovich, I.; Castelletto, S.; Simpson, D. A.; Su, C.-H.; Greentree, A. D.; Prawer, S. Diamond-Based Single-Photon Emitters. *Rep. Prog. Phys.* **2011**, *74*, 076501. https://doi.org/10.1088/0034-4885/74/7/076501.
(13) Atatüre, M.; Englund, D.; Vamivakas, N.; Lee, S.-Y.; Wrachtrup, J. Material Platforms for Spin-Based Photonic Quantum Technologies. *Nat. Rev. Mater.* **2018**, *3* (5), 38–51. https://doi.org/10.1038/s41578-018-0008-9.
(14) Chakraborty, C.; Vamivakas, N.; Englund, D. Advances in Quantum Light Emission from 2D Materials. *Nanophotonics* **2019**, *8* (11), 2017–2032. https://doi.org/10.1515/nanoph-2019-0140.
(15) Azzam, S. I.; Parto, K.; Moody, G. Prospects and Challenges of Quantum Emitters in 2D Materials. *Appl. Phys. Lett.* **2021**, *118* (24), 240502. https://doi.org/10.1063/5.0054116.
(16) Toth, M.; Aharonovich, I. Single Photon Sources in Atomically Thin Materials. *Annu. Rev. Phys. Chem.* **2019**, *70* (1), 123–142. https://doi.org/10.1146/annurev-physchem-042018-052628.
(17) Dastidar, M. G.; Thekkooden, I.; Nayak, P. K.; Bhallamudi, V. P. Quantum Emitters and Detectors Based on 2D van Der Waals Materials. *Nanoscale* **2022**, *14* (14), 5289–5313. https://doi.org/10.1039/D1NR08193D.
(18) Ren, S.; Tan, Q.; Zhang, J. Review on the Quantum Emitters in Two-Dimensional Materials. *J. Semicond.* **2019**, *40* (7), 071903. https://doi.org/10.1088/1674-4926/40/7/071903.
(19) Aharonovich, I.; Englund, D.; Toth, M. Solid-State Single-Photon Emitters. *Nat. Photonics* **2016**, *10*, 631–641. https://doi.org/10.1038/nphoton.2016.186.
(20) Chirolli, L.; Burkard, G. Decoherence in Solid-State Qubits. *Adv. Phys.* **2008**, *57*, 225–285. https://doi.org/10.1080/00018730802218067.
(21) Ye, M.; Seo, H.; Galli, G. Spin Coherence in Two-Dimensional Materials. *Npj Comput.*

Mater. **2019**, *5* (1), 1–6. https://doi.org/10.1038/s41524-019-0182-3.
(22) Lee, K. G.; Chen, X. W.; Eghlidi, H.; Kukura, P.; Lettow, R.; Renn, A.; Sandoghdar, V.; Götzinger, S. A Planar Dielectric Antenna for Directional Single-Photon Emission and near-Unity Collection Efficiency. *Nat. Photonics* **2011**, *5* (3), 166–169. https://doi.org/10.1038/nphoton.2010.312.
(23) Branny, A.; Kumar, S.; Proux, R.; Gerardot, B. D. Deterministic Strain-Induced Arrays of Quantum Emitters in a Two-Dimensional Semiconductor. *Nat. Commun.* **2017**, *8* (1), 15053. https://doi.org/10.1038/ncomms15053.
(24) Ziegler, J.; Klaiss, R.; Blaikie, A.; Miller, D.; Horowitz, V. R.; Alemán, B. J. Deterministic Quantum Emitter Formation in Hexagonal Boron Nitride via Controlled Edge Creation. *Nano Lett.* **2019**, *19* (3), 2121–2127. https://doi.org/10.1021/acs.nanolett.9b00357.
(25) Häußler, S.; Bayer, G.; Waltrich, R.; Mendelson, N.; Li, C.; Hunger, D.; Aharonovich, I.; Kubanek, A. Tunable Fiber-Cavity Enhanced Photon Emission from Defect Centers in HBN. *Adv. Opt. Mater.* **2021**, *n/a* (n/a), 2002218. https://doi.org/10.1002/adom.202002218.
(26) Castelletto, S.; Johnson, B. C.; Ivády, V.; Stavrias, N.; Umeda, T.; Gali, A.; Ohshima, T. A Silicon Carbide Room-Temperature Single-Photon Source. *Nat. Mater.* **2014**, *13* (2), 151–156. https://doi.org/10.1038/nmat3806.
(27) Brown, R. H.; Twiss, R. Q. Correlation between Photons in Two Coherent Beams of Light. *Nature* **1956**, *177* (4497), 27–29. https://doi.org/10.1038/177027a0.
(28) Hong, C. K.; Ou, Z. Y.; Mandel, L. Measurement of Subpicosecond Time Intervals between Two Photons by Interference. *Phys. Rev. Lett.* **1987**, *59* (18), 2044–2046. https://doi.org/10.1103/PhysRevLett.59.2044.
(29) Gruber, A.; Dräbenstedt, A.; Tietz, C.; Fleury, L.; Wrachtrup, J.; Borczyskowski, C. von. Scanning Confocal Optical Microscopy and Magnetic Resonance on Single Defect Centers. *Science* **1997**, *276*, 2012–2014. https://doi.org/10.1126/science.276.5321.2012.
(30) Gupta, S.; Yang, J.-H.; Yakobson, B. I. Two-Level Quantum Systems in Two-Dimensional Materials for Single Photon Emission. *Nano Lett.* **2019**, *19*, 408–414. https://doi.org/10.1021/acs.nanolett.8b04159.
(31) Gupta, S.; Shirodkar, S. N.; Kaplan, D.; Swaminathan, V.; Yakobson, B. I. Franck Condon Shift Assessment in 2D MoS 2. *J. Phys. Condens. Matter* **2018**, *30*, 095501. https://doi.org/10.1088/1361-648X/aaa93e.
(32) Lee, Y.; Hu, Y.; Lang, X.; Kim, D.; Li, K.; Ping, Y.; Fu, K.-M. C.; Cho, K. Spin-Defect Qubits in Two-Dimensional Transition Metal Dichalcogenides Operating at Telecom Wavelengths. *Nat. Commun.* **2022**, *13* (1), 7501. https://doi.org/10.1038/s41467-022-35048-0.
(33) Tran, T. T.; Bray, K.; Ford, M. J.; Toth, M.; Aharonovich, I. Quantum Emission from Hexagonal Boron Nitride Monolayers. *Nat. Nanotechnol.* **2016**, *11*, 37–41. https://doi.org/10.1038/nnano.2015.242.
(34) Gottscholl, A.; Kianinia, M.; Soltamov, V.; Orlinskii, S.; Mamin, G.; Bradac, C.; Kasper, C.; Krambrock, K.; Sperlich, A.; Toth, M.; Aharonovich, I.; Dyakonov, V. Initialization and Read-out of Intrinsic Spin Defects in a van Der Waals Crystal at Room Temperature. *Nat. Mater.* **2020**, *19* (5), 540–545. https://doi.org/10.1038/s41563-020-0619-6.
(35) Tran, T. T.; Elbadawi, C.; Totonjian, D.; Lobo, C. J.; Grosso, G.; Moon, H.; Englund, D. R.; Ford, M. J.; Aharonovich, I.; Toth, M. Robust Multicolor Single Photon Emission from Point Defects in Hexagonal Boron Nitride. *ACS Nano* **2016**, *10*, 7331–7338. https://doi.org/10.1021/acsnano.6b03602.
(36) Bourrellier, R.; Meuret, S.; Tararan, A.; Stéphan, O.; Kociak, M.; Tizei, L. H. G.; Zobelli, A. Bright UV Single Photon Emission at Point Defects in H-BN. *Nano Lett.* **2016**, *16*, 4317–4321. https://doi.org/10.1021/acs.nanolett.6b01368.
(37) Kurtsiefer, C.; Mayer, S.; Zarda, P.; Weinfurter, H. Stable Solid-State Source of Single Photons. *Phys. Rev. Lett.* **2000**, *85*, 290–293. https://doi.org/10.1103/PhysRevLett.85.290.

(38) Pelton, M. Modified Spontaneous Emission in Nanophotonic Structures. *Nat. Photonics* **2015**, *9* (7), 427–435. https://doi.org/10.1038/nphoton.2015.103.
(39) Exarhos, A. L.; Hopper, D. A.; Patel, R. N.; Doherty, M. W.; Bassett, L. C. Magnetic-Field-Dependent Quantum Emission in Hexagonal Boron Nitride at Room Temperature. *Nat. Commun.* **2019**, *10* (1), 222. https://doi.org/10.1038/s41467-018-08185-8.
(40) Sontheimer, B. Photodynamics of Quantum Emitters in Hexagonal Boron Nitride Revealed by Low-Temperature Spectroscopy. *Phys. Rev. B* **2017**, *96* (12), 121202. https://doi.org/10.1103/PhysRevB.96.121202.
(41) Wu, F.; Galatas, A.; Sundararaman, R.; Rocca, D.; Ping, Y. First-Principles Engineering of Charged Defects for Two-Dimensional Quantum Technologies. *Phys. Rev. Mater.* **2017**, *1* (7), 071001. https://doi.org/10.1103/PhysRevMaterials.1.071001.
(42) Mendelson, N.; Chugh, D.; Reimers, J. R.; Cheng, T. S.; Gottscholl, A.; Long, H.; Mellor, C. J.; Zettl, A.; Dyakonov, V.; Beton, P. H.; Novikov, S. V.; Jagadish, C.; Tan, H. H.; Ford, M. J.; Toth, M.; Bradac, C.; Aharonovich, I. Identifying Carbon as the Source of Visible Single-Photon Emission from Hexagonal Boron Nitride. *Nat. Mater.* **2021**, *20* (3), 321–328. https://doi.org/10.1038/s41563-020-00850-y.
(43) Abdi, M.; Chou, J.-P.; Gali, A.; Plenio, M. B. Color Centers in Hexagonal Boron Nitride Monolayers: A Group Theory and Ab Initio Analysis. *ACS Photonics* **2018**, *5* (5), 1967–1976. https://doi.org/10.1021/acsphotonics.7b01442.
(44) Turiansky, M. E.; Alkauskas, A.; Bassett, L. C.; Van de Walle, C. G. Dangling Bonds in Hexagonal Boron Nitride as Single-Photon Emitters. *Phys. Rev. Lett.* **2019**, *123* (12), 127401. https://doi.org/10.1103/PhysRevLett.123.127401.
(45) Hayee, F.; Yu, L.; Zhang, J. L.; Ciccarino, C. J.; Nguyen, M.; Marshall, A. F.; Aharonovich, I.; Vučković, J.; Narang, P.; Heinz, T. F.; Dionne, J. A. Revealing Multiple Classes of Stable Quantum Emitters in Hexagonal Boron Nitride with Correlated Optical and Electron Microscopy. *Nat. Mater.* **2020**, *19* (5), 534–539. https://doi.org/10.1038/s41563-020-0616-9.
(46) Grosso, G.; Moon, H.; Lienhard, B.; Ali, S.; Efetov, D. K.; Furchi, M. M.; Jarillo-Herrero, P.; Ford, M. J.; Aharonovich, I.; Englund, D. Tunable and High-Purity Room Temperature Single-Photon Emission from Atomic Defects in Hexagonal Boron Nitride. *Nat. Commun.* **2017**, *8*, 705. https://doi.org/10.1038/s41467-017-00810-2.
(47) Noh, G.; Choi, D.; Kim, J.-H.; Im, D.-G.; Kim, Y.-H.; Seo, H.; Lee, J. Stark Tuning of Single-Photon Emitters in Hexagonal Boron Nitride. *Nano Lett.* **2018**, *18* (8), 4710–4715. https://doi.org/10.1021/acs.nanolett.8b01030.
(48) He, Y.-M.; Clark, G.; Schaibley, J. R.; He, Y.; Chen, M.-C.; Wei, Y.-J.; Ding, X.; Zhang, Q.; Yao, W.; Xu, X.; Lu, C.-Y.; Pan, J.-W. Single Quantum Emitters in Monolayer Semiconductors. *Nat. Nanotechnol.* **2015**, *10*, 497–502. https://doi.org/10.1038/nnano.2015.75.
(49) Palacios-Berraquero, C.; Barbone, M.; Kara, D. M.; Chen, X.; Goykhman, I.; Yoon, D.; Ott, A. K.; Beitner, J.; Watanabe, K.; Taniguchi, T.; Ferrari, A. C.; Atatüre, M. Atomically Thin Quantum Light-Emitting Diodes. *Nat. Commun.* **2016**, *7* (1), 12978. https://doi.org/10.1038/ncomms12978.
(50) Palacios-Berraquero, C.; Kara, D. M.; Montblanch, A. R.-P.; Barbone, M.; Latawiec, P.; Yoon, D.; Ott, A. K.; Loncar, M.; Ferrari, A. C.; Atatüre, M. Large-Scale Quantum-Emitter Arrays in Atomically Thin Semiconductors. *Nat. Commun.* **2017**, *8* (1), 15093. https://doi.org/10.1038/ncomms15093.
(51) Chakraborty, C.; Kinnischtzke, L.; Goodfellow, K. M.; Beams, R.; Vamivakas, A. N. Voltage-Controlled Quantum Light from an Atomically Thin Semiconductor. *Nat. Nanotechnol.* **2015**, *10* (6), 507–511. https://doi.org/10.1038/nnano.2015.79.
(52) Srivastava, A.; Sidler, M.; Allain, A. V.; Lembke, D. S.; Kis, A.; Imamoğlu, A. Optically Active Quantum Dots in Monolayer WSe 2. *Nat. Nanotechnol.* **2015**, *10* (6), 491–496. https://doi.org/10.1038/nnano.2015.60.
(53) Koperski, M.; Nogajewski, K.; Arora, A.; Cherkez, V.; Mallet, P.; Veuillen, J.-Y.; Marcus, J.; Kossacki, P.; Potemski, M. Single Photon Emitters in Exfoliated WSe 2 Structures. *Nat. Nanotechnol.* **2015**, *10* (6), 503–506. https://doi.org/10.1038/nnano.2015.67.

(54) Rosenberger, M. R.; Dass, C. K.; Chuang, H.-J.; Sivaram, S. V.; McCreary, K. M.; Hendrickson, J. R.; Jonker, B. T. Quantum Calligraphy: Writing Single-Photon Emitters in a Two-Dimensional Materials Platform. *ACS Nano* **2019**, *13* (1), 904–912. https://doi.org/10.1021/acsnano.8b08730.
(55) Li, X.; Wang, W.; Ma, X. Quantum Photon Sources in WSe2 Monolayers Induced by Weakly Localized Strain Fields. *J. Phys. Chem. C* **2022**, *126* (47), 20057–20064. https://doi.org/10.1021/acs.jpcc.2c06148.
(56) Wang, K.; Puretzky, A. A.; Hu, Z.; Srijanto, B. R.; Li, X.; Gupta, N.; Yu, H.; Tian, M.; Mahjouri-Samani, M.; Gao, X.; Oyedele, A.; Rouleau, C. M.; Eres, G.; Yakobson, B. I.; Yoon, M.; Xiao, K.; Geohegan, D. B. Strain Tolerance of Two-Dimensional Crystal Growth on Curved Surfaces. *Sci. Adv.* **2019**, *5* (5), eaav4028. https://doi.org/10.1126/sciadv.aav4028.
(57) Gupta, S.; Yu, H.; Yakobson, B. I. Designing 1D Correlated-Electron States by Non-Euclidean Topography of 2D Monolayers. *Nat. Commun.* **2022**, *13* (1), 3103. https://doi.org/10.1038/s41467-022-30818-2.
(58) Zhao, H.; Pettes, M. T.; Zheng, Y.; Htoon, H. Site-Controlled Telecom-Wavelength Single-Photon Emitters in Atomically-Thin MoTe2. *Nat. Commun.* **2021**, *12* (1), 6753. https://doi.org/10.1038/s41467-021-27033-w.
(59) Klein, J.; Sigl, L.; Gyger, S.; Barthelmi, K.; Florian, M.; Rey, S.; Taniguchi, T.; Watanabe, K.; Jahnke, F.; Kastl, C.; Zwiller, V.; Jöns, K. D.; Müller, K.; Wurstbauer, U.; Finley, J. J.; Holleitner, A. W. Engineering the Luminescence and Generation of Individual Defect Emitters in Atomically Thin MoS2. *ACS Photonics* **2021**, *8* (2), 669–677. https://doi.org/10.1021/acsphotonics.0c01907.
(60) Branny, A.; Wang, G.; Kumar, S.; Robert, C.; Lassagne, B.; Marie, X.; Gerardot, B. D.; Urbaszek, B. Discrete Quantum Dot like Emitters in Monolayer MoSe2: Spatial Mapping, Magneto-Optics, and Charge Tuning. *Appl. Phys. Lett.* **2016**, *108* (14), 142101. https://doi.org/10.1063/1.4945268.
(61) Baek, H.; Brotons-Gisbert, M.; Koong, Z. X.; Campbell, A.; Rambach, M.; Watanabe, K.; Taniguchi, T.; Gerardot, B. D. Highly Energy-Tunable Quantum Light from Moiré-Trapped Excitons. *Sci. Adv.* **2020**, *6* (37), eaba8526. https://doi.org/10.1126/sciadv.aba8526.
(62) Tonndorf, P.; Schwarz, S.; Kern, J.; Niehues, I.; Pozo-Zamudio, O. D.; Dmitriev, A. I.; Bakhtinov, A. P.; Borisenko, D. N.; Kolesnikov, N. N.; Tartakovskii, A. I.; Vasconcellos, S. M. de; Bratschitsch, R. Single-Photon Emitters in GaSe. *2D Mater.* **2017**, *4* (2), 021010. https://doi.org/10.1088/2053-1583/aa525b.
(63) Tran, T. T.; Choi, S.; Scott, J. A.; Xu, Z.-Q.; Zheng, C.; Seniutinas, G.; Bendavid, A.; Fuhrer, M. S.; Toth, M.; Aharonovich, I. Room-Temperature Single-Photon Emission from Oxidized Tungsten Disulfide Multilayers. *Adv. Opt. Mater.* **2017**, *5* (5), 1600939. https://doi.org/10.1002/adom.201600939.
(64) Luo, Y.; Liu, N.; Li, X.; Hone, J. C.; Strauf, S. Single Photon Emission in WSe 2 up 160\hspace0.167emK by Quantum Yield Control. *2D Mater.* **2019**, *6* (3), 035017. https://doi.org/10.1088/2053-1583/ab15fe.
(65) Parto, K.; Azzam, S. I.; Banerjee, K.; Moody, G. Defect and Strain Engineering of Monolayer WSe2 Enables Site-Controlled Single-Photon Emission up to 150 K. *Nat. Commun.* **2021**, *12* (1), 3585. https://doi.org/10.1038/s41467-021-23709-5.
(66) Chakraborty, C.; Goodfellow, K. M.; Dhara, S.; Yoshimura, A.; Meunier, V.; Vamivakas, A. N. Quantum-Confined Stark Effect of Individual Defects in a van Der Waals Heterostructure. *Nano Lett.* **2017**, *17* (4), 2253–2258. https://doi.org/10.1021/acs.nanolett.6b04889.
(67) Hötger, A.; Klein, J.; Barthelmi, K.; Sigl, L.; Sigger, F.; Männer, W.; Gyger, S.; Florian, M.; Lorke, M.; Jahnke, F.; Taniguchi, T.; Watanabe, K.; Jöns, K. D.; Wurstbauer, U.; Kastl, C.; Müller, K.; Finley, J. J.; Holleitner, A. W. Gate-Switchable Arrays of Quantum Light Emitters in Contacted Monolayer MoS2 van Der Waals Heterodevices. *Nano Lett.* **2021**, *21* (2), 1040–1046. https://doi.org/10.1021/acs.nanolett.0c04222.
(68) Sorokin, P. B.; Yakobson, B. I. Two-Dimensional Diamond—Diamane: Current State

and Further Prospects. *Nano Lett.* **2021**, *21* (13), 5475–5484. https://doi.org/10.1021/acs.nanolett.1c01557.
(69) Erohin, S. V.; Ruan, Q.; Sorokin, P. B.; Yakobson, B. I. Nano-Thermodynamics of Chemically Induced Graphene–Diamond Transformation. *Small* **2020**, *16* (47), 2004782. https://doi.org/10.1002/smll.202004782.
(70) Kochat, V.; Apte, A.; Hachtel, J. A.; Kumazoe, H.; Krishnamoorthy, A.; Susarla, S.; Idrobo, J. C.; Shimojo, F.; Vashishta, P.; Kalia, R.; Nakano, A.; Tiwary, C. S.; Ajayan, P. M. Re Doping in 2D Transition Metal Dichalcogenides as a New Route to Tailor Structural Phases and Induced Magnetism. *Adv. Mater.* **2017**, *29*, 1703754. https://doi.org/10.1002/adma.201703754.
(71) Bertoldo, F.; Ali, S.; Manti, S.; Thygesen, K. S. Quantum Point Defects in 2D Materials - the QPOD Database. *Npj Comput. Mater.* **2022**, *8* (1), 1–16. https://doi.org/10.1038/s41524-022-00730-w.
(72) Frey, N. C.; Akinwande, D.; Jariwala, D.; Shenoy, V. B. Machine Learning-Enabled Design of Point Defects in 2D Materials for Quantum and Neuromorphic Information Processing. *ACS Nano* **2020**, *14* (10), 13406–13417. https://doi.org/10.1021/acsnano.0c05267.
(73) Ping, Y.; Smart, T. J. Computational Design of Quantum Defects in Two-Dimensional Materials. *Nat. Comput. Sci.* **2021**, *1* (10), 646–654. https://doi.org/10.1038/s43588-021-00140-w.
(74) Mitterreiter, E.; Schuler, B.; Micevic, A.; Hernangómez-Pérez, D.; Barthelmi, K.; Cochrane, K. A.; Kiemle, J.; Sigger, F.; Klein, J.; Wong, E.; Barnard, E. S.; Watanabe, K.; Taniguchi, T.; Lorke, M.; Jahnke, F.; Finley, J. J.; Schwartzberg, A. M.; Qiu, D. Y.; Refaely-Abramson, S.; Holleitner, A. W.; Weber-Bargioni, A.; Kastl, C. The Role of Chalcogen Vacancies for Atomic Defect Emission in MoS2. *Nat. Commun.* **2021**, *12* (1), 3822. https://doi.org/10.1038/s41467-021-24102-y.
(75) Naydenov, B.; Kolesov, R.; Batalov, A.; Meijer, J.; Pezzagna, S.; Rogalla, D.; Jelezko, F.; Wrachtrup, J. Engineering Single Photon Emitters by Ion Implantation in Diamond. *Appl. Phys. Lett.* **2009**, *95* (18), 181109. https://doi.org/10.1063/1.3257976.
(76) Mitterreiter, E.; Schuler, B.; Cochrane, K. A.; Wurstbauer, U.; Weber-Bargioni, A.; Kastl, C.; Holleitner, A. W. Atomistic Positioning of Defects in Helium Ion Treated Single-Layer MoS2. *Nano Lett.* **2020**, *20* (6), 4437–4444. https://doi.org/10.1021/acs.nanolett.0c01222.
(77) Ngoc My Duong, H.; Nguyen, M. A. P.; Kianinia, M.; Ohshima, T.; Abe, H.; Watanabe, K.; Taniguchi, T.; Edgar, J. H.; Aharonovich, I.; Toth, M. Effects of High-Energy Electron Irradiation on Quantum Emitters in Hexagonal Boron Nitride. *ACS Appl. Mater. Interfaces* **2018**, *10* (29), 24886–24891. https://doi.org/10.1021/acsami.8b07506.
(78) Gao, X.; Pandey, S.; Kianinia, M.; Ahn, J.; Ju, P.; Aharonovich, I.; Shivaram, N.; Li, T. Femtosecond Laser Writing of Spin Defects in Hexagonal Boron Nitride. *ACS Photonics* **2021**, *8* (4), 994–1000. https://doi.org/10.1021/acsphotonics.0c01847.
(79) Kozawa, D.; Li, S. X.; Ichihara, T.; Rajan, A. G.; Gong, X.; He, G.; Koman, V. B.; Zeng, Y.; Kuehne, M.; Silmore, K. S.; Parviz, D.; Liu, P.; Liu, A. T.; Faucher, S.; Yuan, Z.; Warner, J.; Blankschtein, D.; Strano, M. S. Discretized Hexagonal Boron Nitride Quantum Emitters and Their Chemical Interconversion. *Nanotechnology* **2023**, *34* (11), 115702. https://doi.org/10.1088/1361-6528/aca984.
(80) Su, C.; Zhang, F.; Kahn, S.; Shevitski, B.; Jiang, J.; Dai, C.; Ungar, A.; Park, J.-H.; Watanabe, K.; Taniguchi, T.; Kong, J.; Tang, Z.; Zhang, W.; Wang, F.; Crommie, M.; Louie, S. G.; Aloni, S.; Zettl, A. Tuning Colour Centres at a Twisted Hexagonal Boron Nitride Interface. *Nat. Mater.* **2022**, *21* (8), 896–902. https://doi.org/10.1038/s41563-022-01303-4.
(81) Wang, D.; Sundararaman, R. Substrate Effects on Charged Defects in Two-Dimensional Materials. *Phys. Rev. Mater.* **2019**, *3* (8), 083803. https://doi.org/10.1103/PhysRevMaterials.3.083803.
(82) Shree, S.; Semina, M.; Robert, C.; Han, B.; Amand, T.; Balocchi, A.; Manca, M.; Courtade, E.; Marie, X.; Taniguchi, T.; Watanabe, K.; Glazov, M. M.; Urbaszek, B.

Observation of Exciton-Phonon Coupling in ${\mathrm{MoSe}}_{2}$ Monolayers. *Phys. Rev. B* **2018**, *98* (3), 035302. https://doi.org/10.1103/PhysRevB.98.035302.
(83) Ajayi, O. A.; Ardelean, J. V.; Shepard, G. D.; Wang, J.; Antony, A.; Taniguchi, T.; Watanabe, K.; Heinz, T. F.; Strauf, S.; Zhu, X.-Y.; Hone, J. C. Approaching the Intrinsic Photoluminescence Linewidth in Transition Metal Dichalcogenide Monolayers. *2D Mater.* **2017**, *4* (3), 031011. https://doi.org/10.1088/2053-1583/aa6aa1.
(84) Luo, Y.; Liu, N.; Li, X.; Hone, J. C.; Strauf, S. Single Photon Emission in WSe2 up 160 K by Quantum Yield Control. *2D Mater.* **2019**, *6* (3), 035017. https://doi.org/10.1088/2053-1583/ab15fe.
(85) Rhodes, D.; Chae, S. H.; Ribeiro-Palau, R.; Hone, J. Disorder in van Der Waals Heterostructures of 2D Materials. *Nat. Mater.* **2019**, *18* (6), 541–549. https://doi.org/10.1038/s41563-019-0366-8.
(86) Narun, L. R.; Fishman, R. E. K.; Shulevitz, H. J.; Patel, R. N.; Bassett, L. C. Efficient Analysis of Photoluminescence Images for the Classification of Single-Photon Emitters. arXiv December 10, 2021. https://doi.org/10.48550/arXiv.2112.05654.
(87) Kudyshev, Z. A.; Bogdanov, S. I.; Isacsson, T.; Kildishev, A. V.; Boltasseva, A.; Shalaev, V. M. Rapid Classification of Quantum Sources Enabled by Machine Learning. *Adv. Quantum Technol.* **2020**, *3* (10), 2000067. https://doi.org/10.1002/qute.202000067.
(88) Bathen, M. E.; Vines, L. Manipulating Single-Photon Emission from Point Defects in Diamond and Silicon Carbide. *Adv. Quantum Technol.* **2021**, *4* (7), 2100003. https://doi.org/10.1002/qute.202100003.